

# Dynamic Response of a Gyrostabilized Platform Using a Digital Accelerometer during Erection

BURTON BOXENHORN\*

Massachusetts Institute of Technology, Cambridge, Mass.

With the advent of digital computers for inertial guidance systems, it has become convenient for the guidance accelerometers to have quantized, i.e., digital, outputs. The subsequent use of these digital accelerometers to erect the stable platform to the local vertical will result in a discontinuous type of behavior and finally in a limit cycle. An analysis was made of the transient response of a stable platform when being erected with a digital accelerometer. A simple method is presented for calculating the trajectories of the erection system in the phase plane, and finally for obtaining the transient response. Using normalized parameters, the range of frequency and rms amplitude of the final limit cycle is obtained. Other effects are discussed.

## Nomenclature

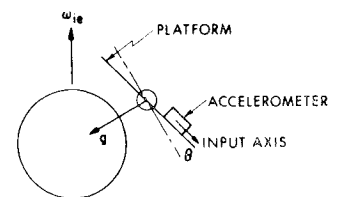
$a$	= asymmetry, numerical difference between maximum $\phi$ of symmetric limit cycle and maximum $\phi$ of asymmetric limit cycle
$c$	= dimensionless parameter
$F$	= normalized frequency, ratio of lead time constant and limit cycle period
$g$	= acceleration of gravity, ft/sec <sup>2</sup>
$K$	= loop gain, rad/ft
$s$	= complex frequency in Laplace transform notation, 1/sec
$T$	= lead time constant, sec
$t$	= time, sec
$t_p$	= limit cycle period, sec
$\Delta V$	= digital accelerometer output impulse weight, fps
$\theta, \theta_{ep}$	= output angle of platform with respect to the horizontal plane of the earth
$\omega_{ie}$	= platform angular rate with respect to inertial space
$\omega_{ie}$	= angular rate of the earth with respect to inertial space
$\omega_{ep}$	= angular rate of the platform with respect to the earth
$\tau$	= normalized time
$\phi$	= normalized angle or amplitude
$\phi_{rms}$	= rms amplitude
$\zeta$	= damping ratio
$(\cdot)$	= differentiation with respect to time, or normalized time
$(\cdot)_i$	= initial value
$\Delta t$	= time increment between $\Delta V$ pulses
$t_{\Delta V}$	= $t_0 + \Delta t$

## Introduction

THE erection of a stable platform of an inertial guidance system to the local vertical is accomplished by nulling the input of an accelerometer by torquing the gyros of the stable platform. The dynamic analysis of this process is simple and straightforward when the accelerometer provides a continuous analog output. With the advent of the use of digital computers in conjunction with inertial guidance systems, it becomes convenient for the accelerometer output to be quantized. This type of accelerometer is called here a digital accelerometer. The subsequent use of a digital accelerometer in erecting the platform will result in a discontinuous type of behavior, and finally in a limit cycle.

It is the purpose here to present an analysis of the transient response of the stable platform when being erected with a digital

Fig. 1 Sketch of platform with accelerometer.



tal accelerometer. A simple method is presented for calculating the trajectories of the system in the phase plane and for obtaining the transient response. Using normalized parameters, several examples are worked out, and some general characteristics of the final limit cycle are presented.

## The Problem

A sketch of the system is shown in Fig. 1. For simplicity in drawing, the platform is shown in Fig. 1 with its axis orthogonal to  $\omega_{ie}$ . Let us think first in terms of a continuous system. The accelerometer output is modified by compensation networks. The resulting current is fed to the gyro torque generator, which causes the stable platform to rotate in inertial space at a rate  $\omega_{ip}$ . Since the platform is on a rotating earth, the angular rate of the platform with respect to the earth  $\omega_{ep}$  is the difference between platform inertial rate and earth rate. The integral of  $\omega_{ep}$  with respect to time gives the platform angle  $\theta_{ep}$  (hereafter referred to simply as  $\theta$ ).

Any resulting angle  $\theta$  introduces a component of gravity equal to  $g \sin \theta$  as an input to the accelerometer. For small  $\theta$  it becomes  $g\theta$ . This component is fed back negatively to null the accelerometer input and to produce  $\theta = 0$ . The mechanics of this type of operation are discussed in greater detail in Ref. 1.

Turning now to the system using a digital accelerometer, its operation is very similar to the analog system described previously, with the exception that the accelerometer output is a train of pulses. A digital accelerometer is an integrating ac-

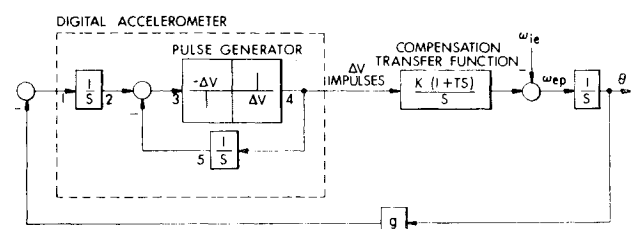


Fig. 2 Erection loop with digital accelerometer.

Received February 18, 1964; revision received September 11, 1964. This work was sponsored by the Special Projects Office (Bureau of Naval Weapons), Department of the Navy, under Contract NOrd 17366 (FBM). The author would like to thank Benedict Olson for suggesting this topic, Richard Haltmaier for providing the opportunity to work on it, and VanderVelde for his very helpful suggestions.

\* Staff Engineer, Instrumentation Laboratory.

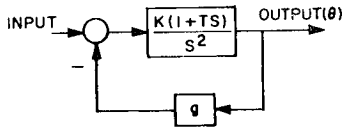


Fig. 3 Linear analog of erection loop.

celerometer; that is, it puts out a pulse each time the integral of the acceleration is a certain value. The complete block diagram for the erection system is shown in Fig. 2.

The digital accelerometer is represented by two integrators and a pulse generator. Looking at Fig. 2, the acceleration input at 1 is integrated until a value at 2 equal to a fixed velocity increment  $\Delta V$  is produced. The pulse generator then produces an impulse of weight  $\Delta V$ . This impulse is the accelerometer output. The impulse is also fed to another integrator whose output is a step. This step is fed back negatively at 5 to the pulse generator input. This resets the pulse generator to zero. Therefore, the input-output relationship for the digital accelerometer (between 1 and 4) is that an impulse is produced of weight  $\Delta V$  every time the increment of the integral of the input acceleration is equal to  $\Delta V$ .

The output impulses are fed to the compensation, whose transfer function is shown in Fig. 2. When  $\theta$  is large, these impulses are produced at a rapid rate, and the system can be considered to be continuous, with the block diagram shown in Fig. 3. As the platform is erected and  $\theta$  approaches zero, the impulses come further and further apart, and the quantized nature of the system becomes predominant. The purpose here is to investigate the behavior of the system at small angles when the system is acting discontinuously.

### Analysis

The following assumptions are made: 1) there is no coupling between the axes of the stable platform, so that a single axis can be considered at a time; and 2) the dynamics of the situation can be considered to be completely represented by the block diagram shown in Fig. 2.

Under the previous assumptions, a straightforward phase-plane analysis can be made. At first, earth rate  $\omega_{ie}$  will be assumed to be zero. Considering Fig. 2, the response will be computed around the loop. Starting at the accelerometer output, the response of the system output ( $\theta$ ) to an impulse of weight  $\Delta V$  is computed. This response, in Laplace transform notation, is

$$\theta(s) = \Delta VK[(1/s^2) + (T/s)] \quad (1)$$

The time response is then

$$\Delta\theta(t) = \Delta VK(t + T) \quad (2)$$

This is sketched in Fig. 4.

The preceding equation gives the incremental response of the system to an impulse of  $\Delta V$ . The result is a jump in  $\theta$  and a jump in the rate  $\dot{\theta}$ . Equation (2) can be written with more significance as

$$\Delta\theta = K\Delta VT \quad (3a)$$

$$\Delta\dot{\theta} = \Delta VK \quad (3b)$$

Continuing around the loop, a  $\Delta V$  impulse is produced when

$$-\Delta V = \int_{t_0}^{t_{\Delta V}} g\theta dt \quad (4)$$

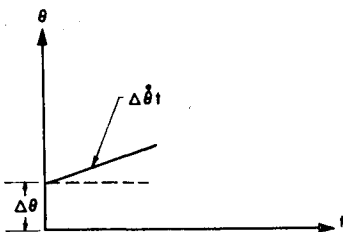


Fig. 4 Response of system to pulse of  $\Delta V$ .

Table 1 Summary of signs when an impulse is produced

Quadrant	Item				
	$\theta$	$\dot{\theta}$	$\Delta V$	$\Delta\theta$	$\Delta\dot{\theta}$
I	+	+	-	-	-
II	+	-	+	+	+
III	-	-	+	+	+
IV	-	+	-	-	-

That is, the acceleration is integrated until an impulse is produced. Now from Eq. (2), between each impulse, the motion of  $\theta(t)$  is linear (see Fig. 5). Then

$$\theta(t) = \theta_i + \dot{\theta}t \quad 0 \leq t \leq \Delta t \quad (5)$$

Substituting Eq. (5) into Eq. (4), and integrating,

$$-\Delta V = g \int_0^{\Delta t} (\theta_i + \dot{\theta}t) dt = g \left[ \theta_i t + \frac{\dot{\theta}t^2}{2} \right]_{0 \leq t \leq \Delta t} \times \quad (6)$$

In the phase plane, time is implicit. Then, eliminating  $t$  between Eqs. (5) and (6) and collecting terms, a final switching function is obtained

$$\dot{\theta} = -(g/2\Delta V)[\theta^2 - \theta_i^2] \quad (7)$$

It is the simplicity of the preceding switching function that makes this analysis practicable. Equation (7) represents a single parabola

$$\dot{\theta} = -(g/2\Delta V)\theta^2 \quad (8)$$

which is shifted up and down by the constant amount  $g\theta_i^2/2\Delta V$ . That is,  $\theta_i$  is a constant between impulses.

### Discussion of Analysis

Equations (3) and (7) are all that are necessary to plot a trajectory in the phase plane. As an aid to the understanding of what follows, Table 1 presents a summary of the signs.

Plotting a phase trajectory proceeds as follows. If the system starts in the first quadrant with some initial value of  $\theta$  and  $\dot{\theta}$ , then, by Eq. (4), it will integrate out a negative  $\Delta V$  impulse. This will produce, by Eq. (3), a negative  $\Delta\theta$  and  $\Delta\dot{\theta}$ . All possible such combinations are shown in Table 1.

Figure 6 shows a sketch of the phase plane with the family of switching curves from Eq. (7). If initially the system is at point 0, then the trajectory is from 0 to 1. At that point the switching parabola corresponding to  $\theta_i$  equal to  $\theta_0$  is reached, and an impulse is generated by the accelerometer. This produces a negative increment of  $\Delta\theta$  and  $\Delta\dot{\theta}$ , as indicated in Table 1, and the trajectory jumps from point 1 to point 2. Note that this increment takes no time, according to this model. After point 2, the system continues at a lower rate to point 3 where it hits the switching parabola corresponding to  $\theta_i$  equal to  $\theta_2$ . It then jumps an increment  $\Delta\theta$  and  $\Delta\dot{\theta}$  to point 4. This procedure continues until a limit cycle is established.

When the trajectory passes through  $\theta = 0$ , the correct switching parabola is the one whose  $\theta_i$  is the negative of the  $\theta_i$  of that particular trajectory. This case is shown in Fig. 6 when establishing point 5, which is in the third quadrant, but the switching parabola is chosen to correspond to  $\theta_i = -\theta_4$ .

### General Results

An examination of the kind of response obtained by this system was performed by first normalizing the pertinent equations and then presenting the results of a graphical analysis of

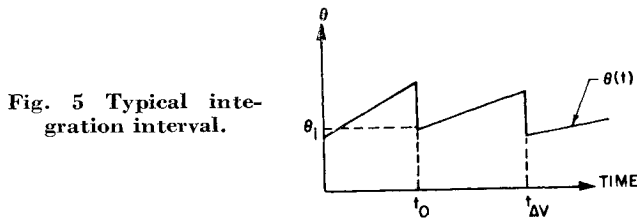


Fig. 5 Typical integration interval.

the resulting normalized equations. The following dimensionless forms are defined:

$$\phi = \theta / |\Delta VKT| \quad (9a)$$

$$\tau = t/T \quad (9b)$$

$$\dot{\phi} = d\phi/d\tau = T d\phi/dt \quad (9c)$$

Equation (2) becomes

$$\Delta\phi(\tau) = \pm(\tau + 1) \quad (10)$$

and Eq. (3) becomes:

$$\Delta\phi = \pm 1 \quad (11a)$$

$$\Delta\dot{\phi} = \pm 1 \quad (11b)$$

Equation (5) becomes

$$\phi(\tau) = \phi_i + \dot{\phi}\tau \quad (12)$$

and Eq. (7) becomes

$$\dot{\phi} = \pm c[\phi^2 - \phi_i^2] \quad (13)$$

where

$$c = gKT^2/2 \quad (14)$$

This normalizes the equations except for the factor  $c$ . Perhaps a better form of writing Eqs. (11) and (13) is

$$\Delta\phi = \pm 1 \quad (15a)$$

$$\Delta(\dot{\phi}/c) = 1/c \quad (15b)$$

$$(\dot{\phi}/c) = \pm [\phi^2 - \phi_i^2] \quad (16)$$

This form has the advantage of requiring the plotting of but one parabola. However,  $c$  is still a variable. Investigating the case where  $c = 1$  makes the equations particularly simple and has a very real practical significance.

Examining Fig. 3, which represents the nearly continuous behavior of the system when  $\theta$  is not near zero, the closed-loop transfer function can be written as

$$\frac{K[1 + Ts]}{s^2 + gKTs + Kg} \quad (17)$$

The damping ratio  $\zeta$  is then

$$\zeta = T(gK)^{1/2}/2 \quad (18)$$

A reasonable value of  $\zeta$ , from the point of view of stability, and, to a certain extent, for minimum settling time (see Ref. 2), is  $\zeta = (2)^{1/2}/2$ . Using this value for  $\zeta$ , Eq. (18) becomes

$$c = gKT^2/2 = 1 \quad (19)$$

Thus, the case for  $c$  equaling unity is not only the simplest case to analyze, but it is also the most probable practical value.

Using the value of  $c = 1$ , a graphical analysis was performed. The object of this analysis was to obtain general results for the limit cycle trajectory in the form of limit cycle frequency and rms value of the amplitude. An example of a transient response was also worked out, and these results are also shown. The results of the graphical analysis are discussed next.

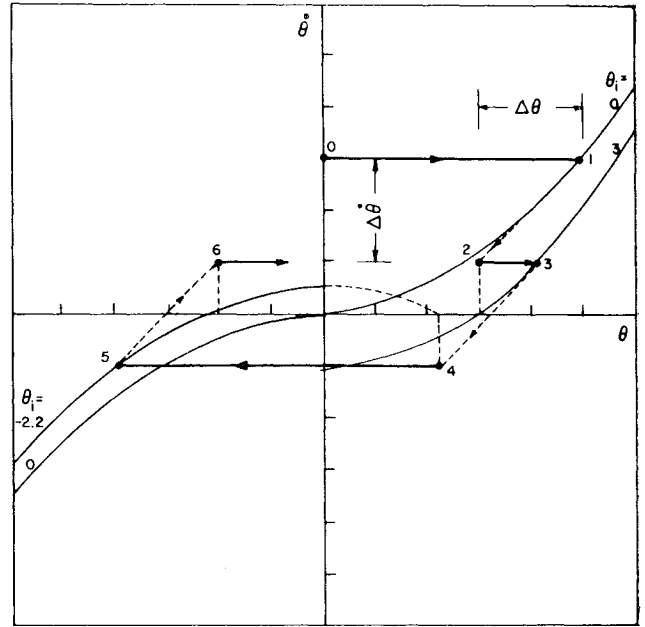


Fig. 6 Sketch of phase-plane trajectory.

### Results of Graphical Analysis

Figures 7 through 13 show the results. Figure 7 shows a typical trajectory. Starting at (5, 0), the trajectory proceeds as shown. The switching parabola ( $\dot{\phi} = \pm\phi^2$ ) is also shown in Fig. 7. In constructing the phase-plane trajectory, it is not necessary to make more than one plot of the switching parabola. This plot is drawn on vellum and is then slid up and down to generate Eq. (16) as needed. Thus, once the switching parabola is plotted, the rest of the geometry is made up of straight line segments. Figure 8 shows the corresponding transient response. This transient response has been plotted using Eq. (12) and normalized Eq. (6).

All trajectories finally form a limit cycle about the origin. Figure 9 shows the bounds of the family of possible limit cycles. The particular limit cycle is analytically a function of the initial conditions. Introducing the parameter  $a$  for the asymmetry of the limit cycle, when  $a = 0$ , the limit cycle is

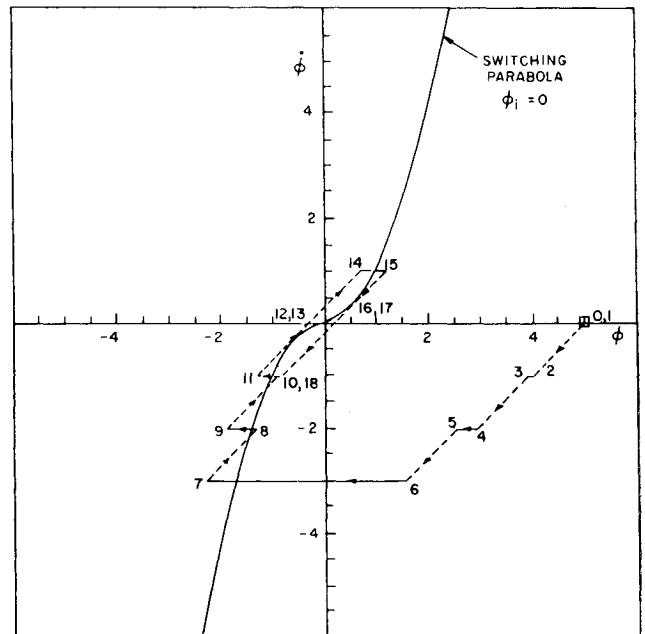


Fig. 7 Trajectories in phase plane,  $c = 1$ .

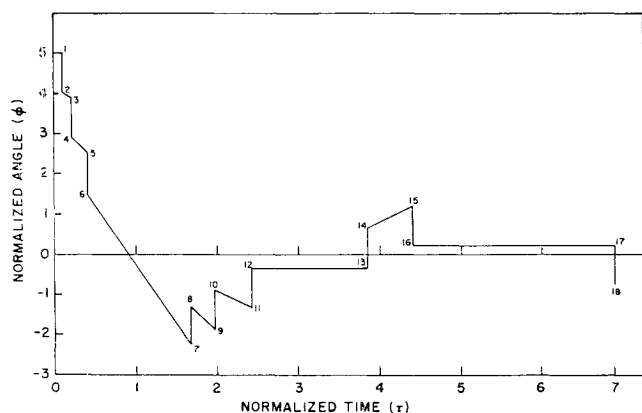


Fig. 8 Transient response from phase-plane trajectories,  $c = 1$ .

symmetric, as shown in Fig. 9. The value of  $a$  is equal to the difference between the maximum  $\phi$  of the symmetric limit cycle and the maximum  $\phi$  of the skewed limit cycle. As  $a$  becomes larger, the limit cycle trajectory shifts upward (or downward; every limit cycle discussed has a mirror image), so that the transient response, shown in Fig. 10, is skewed upward. However, when  $a > 0.46$ , the situation is no longer a rotation about a simple closed path. Instead, between  $0.46 < a < 0.5$ , the trajectory forms a complex limit cycle, as shown in Fig. 11, where the limit cycle trajectory overlaps on itself and encircles the origin more than once. A sample response for such a case is shown for  $a = 0.47$  in Fig. 12. Note that six impulses are required per cycle in Fig. 12, whereas for the simple trajectories, as shown in Fig. 10, only two are required, except for  $a = 0.5$ , where there are four. However, the trajectory for  $a = 0.5$  is, in a sense, a singularity, since the system returns to a simple type of limit cycle trajectory at this point.

From the data of Fig. 10, it is possible to compute the normalized frequency ( $F$ ) and the rms value of the amplitude

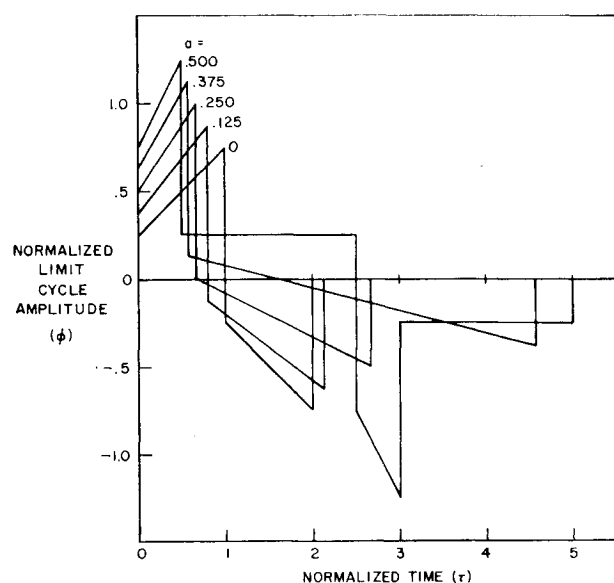


Fig. 10 Limit cycle response as a function of asymmetry  $a$ ,  $c = 1$ .

for each value of  $a$ . The rms amplitude is defined as

$$\phi_{rms} \equiv \left[ F \int_0^{1/F} \phi^2 d\tau \right]^{1/2} \quad (20a)$$

$$F \equiv T/t_p = T/\text{period} \quad (20b)$$

The results are shown in Fig. 13. No attempt was made when plotting Fig. 13 to present results for  $0.46 < a < 0.5$ . It is interesting to note that the equation for  $F$  is

$$F = -2a^2 + \frac{1}{2} \quad 0 \leq a \leq 0.46 \quad (21)$$

Now the question of how to handle earth rate can be answered. If there is a fixed value of  $\omega_{ie}$  at the summing point shown in Fig. 2, then the effect will be to make the stable platform rotate with respect to the earth at the rate  $\dot{\theta} = \omega_{ie}$  and produce a corresponding angle  $\theta$ . So far as the phase-plane analysis is

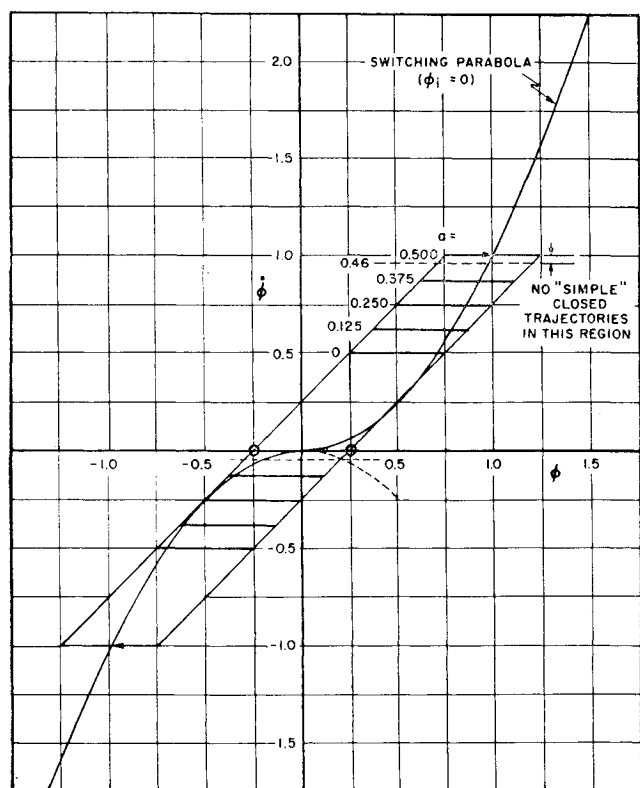


Fig. 9 Limit cycle trajectory in phase plane,  $c = 1$ .

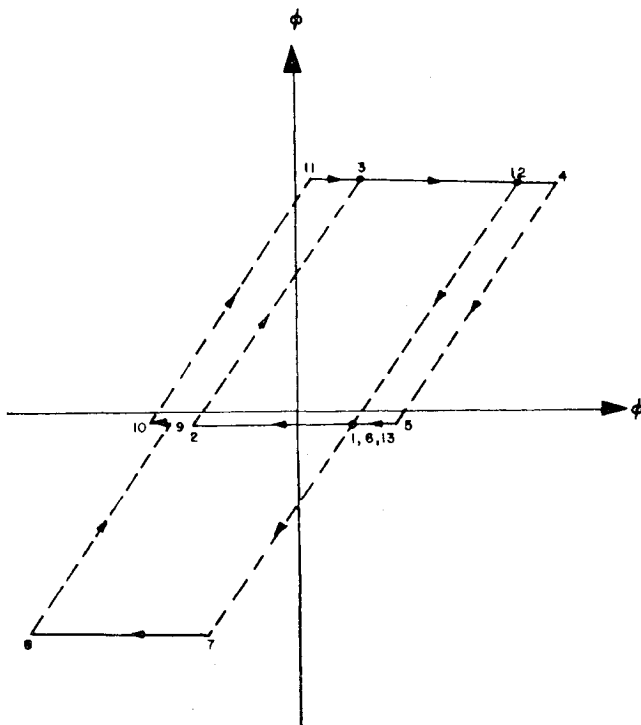


Fig. 11 Sketch of sample complex trajectory  $0.46 < a < 0.5$ ,  $c = 1$ .

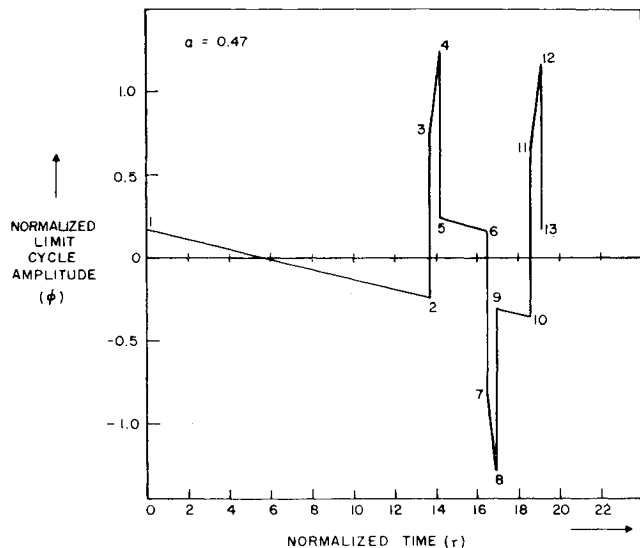


Fig. 12 Example of complex limit cycle response when  $0.46 < a < 0.5$ ,  $c = 1$ .

concerned, this will appear, at a time equal to zero, as an initial value for  $\dot{\theta}$ , added onto whatever other initial value is introduced. The trajectory then proceeds as before, making the effect of  $\omega_{ie}$  on the phase-plane trajectory simply a shift in the initial conditions.

However, physically, it is mostly this factor that will determine the final limit cycle. The torquing current can only change in finite increments due to the impulse, whereas the corresponding component of earth rate is continuous. Thus, there is always a net amount of velocity left over which will cause it to have different limit cycles, i.e.,  $a$  will vary. But note that  $a = 0.5$  is a singularity in the sense that this requires  $\omega_{ie} = 0$ , whereas the character of the limit cycle changes suddenly at that point. Thus,  $a = 0.5$  is physically impossible.

### Further Discussion

The question of course arises as to whether the compensation network chosen is of most practical interest. The answer is that, to be able to erect a system in the presence of earth rate error, it is necessary to have one integration. A minimum of one zero is necessary to stabilize the system. The compensation assumed here is then the minimum necessary to have a self-erecting system. It is possible that, for a number of reasons, additional poles may be added to the compensa-

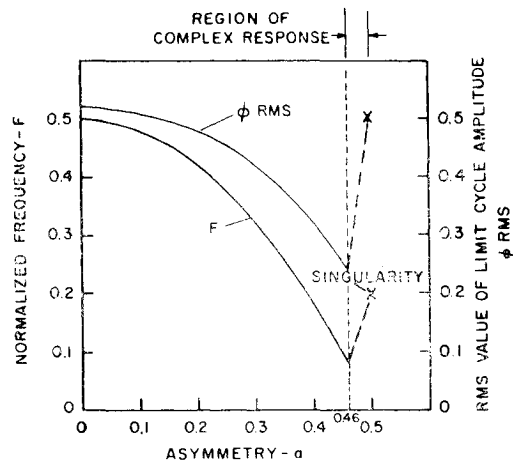


Fig. 13 Limit cycle rms amplitude and frequency vs asymmetry,  $c = 1$ .

tion. The system is then no longer second order, and the analysis developed here can not be applied. However, if the additional poles are far enough removed from the zero, say by a factor of 10, the results obtained by neglecting them will be reasonably valid, at least for the limit cycle.

This analysis can be extended to other cases fairly readily, so long as the second-order nature of the system is retained. For instance, accelerometer dead zone can be handled, as well as different quantization levels in the gyro torquing current.

### Conclusion

This paper has shown that it is possible to determine the dynamic effect of using a digital accelerometer when erecting a stable platform. Quantitative answers are obtained for the platform limit cycle frequency and the rms amplitude. The resulting equations and curves make the design of the erection loop dynamics particularly simple.

### References

- <sup>1</sup> Markey, W. and Hovorka, J., *The Mechanics of Inertial Position and Heading Indication* (Methuen and Co., Ltd., London, and John Wiley and Sons Inc., New York, 1961), Chap. V.
- <sup>2</sup> Draper, C. S., McKay, W., and Lee, S., *Instrument Engineering (III) Part I* (McGraw-Hill Book Co., Inc., New York, 1955), p. 246, Fig. 32.8.
- <sup>3</sup> Boxenhorn, B., "Dynamic response of a gyro stabilized platform using a digital accelerometer during erection," Massachusetts Institute of Technology, Instrumentation Lab., Rept. E-1390 (1963).